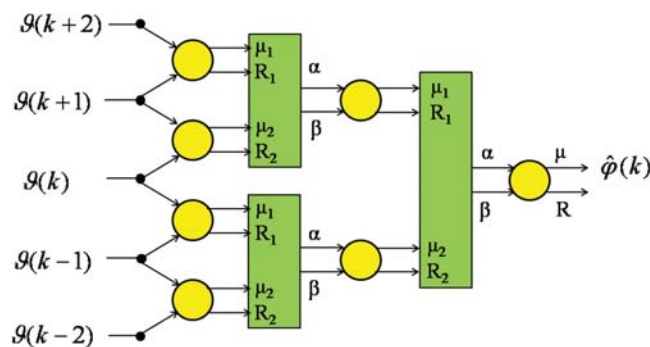


# Hardware-Efficient Phase Estimation for Digital Coherent Transmission With Star Constellation QAM

Volume 2, Number 2, April 2010

Sebastian Hoffmann  
Christian Wördehoff  
Ali Al-Bermani  
Mohamed El-Darawy  
Kidsanapong Puntsri  
Ulrich Rückert  
Reinhold Noé



DOI: 10.1109/JPHOT.2010.2044784  
1943-0655/\$26.00 ©2010 IEEE

# Hardware-Efficient Phase Estimation for Digital Coherent Transmission With Star Constellation QAM

Sebastian Hoffmann,<sup>1</sup> Christian Wördehoff,<sup>1</sup> Ali Al-Bermani,<sup>1</sup>  
Mohamed El-Darawy,<sup>1</sup> Kisanapong Puntsri,<sup>1</sup>  
Ulrich Rückert,<sup>2</sup> and Reinhold Noé<sup>1</sup>

*(Invited Paper)*

<sup>1</sup>University of Paderborn, 33098 Paderborn, Germany

<sup>2</sup>University of Bielefeld, Center of Excellence-Cognitive Interaction Technology (CITEC),  
33501 Bielefeld, Germany

DOI: 10.1109/JPHOT.2010.2044784  
1943-0655/\$26.00 ©2010 IEEE

Manuscript received January 25, 2010; revised February 24, 2010. First published Online March 1, 2010. Current version published March 23, 2010. Corresponding author: S. Hoffmann (e-mail: hoffmann@ont.upb.de).

**Abstract:** In order to build optical transmission systems for 100 Gb/s and above on a single wavelength division multiplexing channel, transition from quadrature phase-shift keying (QPSK) to higher quadrature amplitude modulation (QAM) formats seems to be inevitable. Instead of the usual square constellation QAM, we focus on regular star constellation QAM formats and present a hardware-efficient phase-estimation algorithm that is suitable for all regular star constellations, together with preliminary simulation results.

**Index Terms:** Fiber optics systems, homodyning.

## 1. Introduction

Coherent detection and digital signal processing (DSP) allows employment of advanced transmission techniques like quadrature phase-shift keying (QPSK), multilevel quadrature amplitude modulation (M-QAM), and orthogonal frequency-division multiplexing (OFDM), in combination with polarization multiplex (PM) for optical transmission systems with 112-Gb/s data rate or above. The DSP also permits electronic compensation of intermediate frequency, phase noise [1], and fiber impairments that lead to polarization crosstalk, chromatic dispersion (CD), and polarization-mode dispersion (PMD) [2]. Several real-time experiments using such algorithms for QPSK transmission have already been demonstrated [3], [4]. Even single-chip implementations [5] and modularized implementations with high-speed analog-to-digital converters (ADCs) and a Complementary metal-oxide-semiconductor DSP chip [6] have been presented. On the other hand, research is also still going on with offline experiments that allow the investigation of new algorithms without the need for extensive hardware development [7].

Transition from QPSK to QAM formats would usually focus on square constellation formats because they have the optimum distance for additive noise. The disadvantage of these formats like “three-ring” 16-QAM is that they require a considerable computation effort for phase estimation in order to achieve low bit error ratio (BER) values [8]. Beside additive optical noise, phase noise has to be considered, especially if standard distributed feedback (DFB) lasers with a sum linewidth of 1 MHz or above are employed. The dominance of phase noise may cause a better BER performance to be reached with

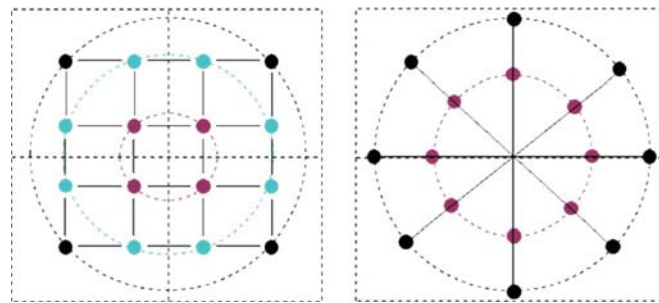


Fig. 1. Two possible 16-QAM constellations. Square constellation (left) and star constellation (right).

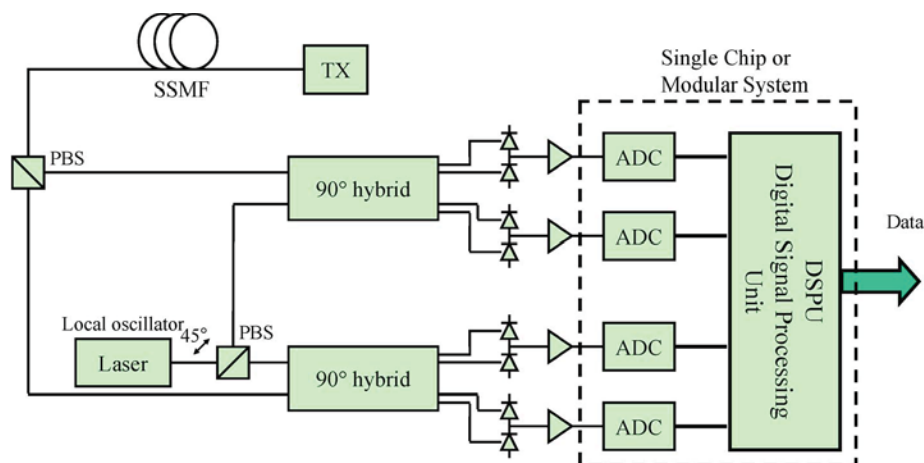


Fig. 2. Coherent receiver structure for polarization multiplex transmission.

alternative QAM constellations. Therefore, we investigate a phase-estimation algorithm that is suitable for certain star constellation formats. The advantage of this algorithm is the simplicity regarding real-time implementations. By the term regular star constellation (RSC), we refer to any QAM format where all constellation points are located on intercepts of circles around the origin (“rings”) and  $R$  lines from the origin with equal angular spacing (“rays”). Binary phase-shift keying (BPSK), QPSK, and other phase-shift keying (PSK) formats like 8-PSK are examples of single-ring RSCs. Their combination with amplitude modulation leads to multiring formats with a higher information content per symbol. Such modulation formats are most efficiently decoded in polar coordinates, and the amplitude modulation can be neglected for angle-based phase estimators like ours.

Fig. 1 shows two possible constellations for 16-QAM: (left) the usual square constellation with point locations on three rings and (right) an alternative star constellation with only two rings. Note that, in the square constellation, middle-ring points do not have an equal angular spacing, which makes phase estimation more difficult. The star constellation can be described as 8-PSK combined with a 1-bit amplitude modulation.

## 2. Coherent Receiver Structure and Real-Time Algorithms

For all modulation formats including OFDM, the coherent receiver with PM and DSP can have the same structure (see Fig. 2): The receiver consists of an optical front end including optical  $90^\circ$  hybrids, optical/electrical conversion, ADCs, and a DSP unit (DSPU). ADCs and DSPU can either be integrated in a single chip to ease interfacing and reduce the footprint [4] or in a modular approach for optimized performance, where ADCs and DSPU can be developed in different technologies for maximum bandwidth and high integration, respectively [5]. In both topologies, the implemented algorithms must allow parallel processing to match system (transmission) standards and technology constraints [9].

The DSPU cannot operate at the sampling clock frequency of the ADC but requires demultiplexing to process the data in  $m$  parallel stages at reduced clock frequencies that are usable for the required signal processing. Therefore, the algorithms should allow parallel processing with an unlimited number  $m$  of demultiplexed channels, which implies that the output of one module is independent of the outputs of the other parallel modules. Another constraint for algorithms used for real-time DSP is hardware efficiency, which also originates from the parallel processing in the DSPU. For example, data recovery and phase estimation usually require coordinate transformations with lookup tables (LUTs). These have to be implemented for each module separately, and if a single coordinate conversion can be avoided, the hardware effort is remarkably reduced.

### 3. Angle-Based Phase Estimation and Polar Coordinate Demodulation

For any QAM transmission without PM, the received symbols after optoelectronic conversion and discretization can be described as a time sequence of complex numbers  $Z(k)$  with the argument  $\psi(k)$  and time index  $k$ . For PM, the received signal from four ADCs can be seen as a pair of two complex numbers  $Z_1(k)$ ,  $Z_2(k)$ , which has (as a vector) to be multiplied by a compensation pair  $X_1(k)$ ,  $X_2(k)$  with arguments  $\psi_1(k)$ ,  $\psi_2(k)$ . We will not go into details on PM and polarization control within this paper, but it should be noted that these angle pair time sequences could also be employed for the described phase-estimation algorithm and that a common phase estimation for both PM channels is advantageous in terms of performance and hardware efficiency.

Because coherent transmission requires a second laser as a local oscillator (LO) on the receiver side, the transmitter (TX) and LO laser can differ in both frequency and phase. This fact leads to an intradyne receiver signal [10] and makes estimation of the intradyne frequency and the phase necessary. For frequency estimation and phase estimation of a regular star QAM transmission without nonlinear phase noise, only the argument of the received symbol is necessary, whereas the magnitudes of the complex numbers only contain the amplitude modulation and fluctuations due to noise. Nevertheless, the usual way to estimate the phase for QPSK proposed by Viterbi and Viterbi (V&V) involves complex calculations [11]. An estimated frequency sufficient for analog LO laser can be obtained from averaged phase increments [12]. Data recovery (also addressed as demodulation in this paper) for an RSC is done most convenient in polar coordinates. Because of the extraordinary high-speed and parallelization requirements, it is advantageous to convert the received signal into polar coordinates with LUTs instead of calculation algorithms for trigonometric functions like the coordinate rotation digital computer [13]. Amplitude modulation data bits can be recovered independent from and in parallel to phase-modulation data bits which require phase estimation and differential encoding. The decoder threshold values for amplitude demodulation can be optimized independent from the phase estimation and demodulation with a slow decision-directed (DD) control structure.

For a synchronous phase demodulator, an estimated phase angle  $\hat{\varphi}(k)$  is subtracted from each received signal angle  $\psi(k)$  in order to compensate for phase noise and residual frequency mismatch. Best results for high-phase-noise requirements can be achieved with estimators that perform a full phase tracking. The estimated phase is usually limited to a certain quadrant; therefore, it is wrapped. Phase unwrapping based on a maximum-likelihood decision is feasible in real time [14], but it is easier to detect the deviations between the physical and wrapped estimated phase, encode it into quadrant jump numbers, and to consider it in the differential decoder that recovers the original data.

### 4. V&V Phase Estimation for QPSK

The phase-estimation algorithm of V&V, similar to our approach, employs a polar coordinate representation of the received signal [11]. It can be employed for any RSC with small adaptations, but in order to simplify notation, we concentrate on QPSK or, more generally, RSCs with four rays; in other words,  $R = 4$ . The received symbol  $Z(k)$  consists of the sent QPSK symbols  $c(k) = \pm 1 \pm j$ , a time-variant phasor  $\exp(j\varphi(k))$  and additional noise  $n(k)$ :

$$Z(k) = |Z(k)| \cdot e^{j\psi(k)} = c(k) \cdot e^{j\varphi(k)} + n(k). \quad (1)$$

The task of the phase estimator is to track the time-variant phase angle time sequence  $\varphi(k)$  resulting from the nonideal behavior of the two lasers TX and LO, despite the additional noise. The frequency mismatch between TX and LO laser leads to intradyne reception and a deterministic component of  $\varphi(k)$  while the sum linewidth of TX and LO causes a random contribution (phase noise). The fourth power of (1) is

$$Z^4(k) = c^4(k) \cdot e^{j4\varphi(k)} + 4c^3(k) \cdot e^{j3\varphi(k)} \cdot n(k) + 6c^2(k) \cdot e^{j2\varphi(k)} \cdot n^2(k) + 4c(k) \cdot e^{j\varphi(k)} \cdot n^3(k) + n^4(k). \quad (2)$$

Because  $c^4(k) = -4$  is constant, the dominating first term of  $Z^4(k)$  in (2) is independent from the QPSK modulation and therefore useful for phase estimation. The other terms of the right-hand side of (2) depend on additive white Gaussian noise (AWGN)  $n(k)$  and can be lumped together into an equivalent AWGN contribution  $n'(k)$  [14]:

$$Z^4(k) \triangleq (-4) \cdot e^{j4\varphi(k)} + n'(k). \quad (3)$$

V&V employed the modulation removal property of  $Z^4(k)$  in their generalized polar coordinate approach based on the product of two separate functions of magnitude and phase [11]. Generalization means in this context that the magnitude might be raised to different integer powers and not only to 4:

$$X(k) = |Z(k)|^u \cdot e^{j4\psi(k)}, \quad (u = 0, 2, 4). \quad (4)$$

As a generalized replacement for  $Z^4(k)$ , the resulting complex signal  $X(k)$  can be averaged (or, more generally, low-pass filtered) in order to remove the noise, and finally, an estimated phase can be obtained from the argument of the complex filter output. The fourfold ambiguity of the complex root can be resolved by a wrapping of the estimated phase [10], [11], [14]. The V&V phase estimator with  $u = 0$  performs a normalization and does not process the magnitude at all, which reduces the hardware effort remarkably. On the other hand, the V&V phase estimator converts the input signal into polar coordinates, performs nonlinear functions of its magnitude and phase, and generates a complex signal  $X(k)$ . Note that  $X(k)$  is represented in Cartesian coordinates for low-pass filtering, but the result is afterward converted into polar coordinates again to obtain the estimated phase. It is desirable to avoid these multiple conversions.

## 5. Angle-Based Phase Estimation for RSC QAM Transmission

In order to avoid multiple coordinate conversions, an angle-based approach can employ the relative position angle  $\vartheta(k)$  of the received symbol defined as follows:

$$\vartheta(k) = \psi(k) \bmod \frac{2\pi}{R} = \frac{1}{R} [\arg(Z^R(k)) \bmod 2\pi]. \quad (5)$$

This position angle could replace  $\psi(k)$  in a V&V phase estimator because of

$$\exp(j \cdot R \cdot \vartheta(k)) = \exp(j \cdot \arg(Z^R(k))) = \exp(j \cdot R \cdot \psi(k)). \quad (6)$$

Therefore,  $\vartheta(k)$  is independent from the phase modulation which makes it an interesting candidate for immediate angle-based phase estimation [15]. In this approach, all input, output, and intermediate values are angles. The phase estimator consists of basic cells that convert pairs of position angles  $\alpha, \beta$  into single averaged position angles  $\mu = f(\alpha, \beta)$ . The partial result from each basic cell is calculated within one DSPU cycle using the sum  $\sigma = \alpha + \beta$  and the difference  $\delta = \alpha - \beta$  of the input values for the final calculation, thus avoiding the complex calculation:

$$\mu = f(\alpha, \beta) = \left( \frac{\sigma}{2} + \frac{\pi}{R} \left[ \frac{|\delta|}{\pi/R} \right] \right) \bmod \frac{2\pi}{R}. \quad (7)$$

Fig. 3 (left) shows the internal structure of the basic cell (bc). The angle output  $\mu$  is generated from the auxiliary quantities  $\sigma$  and  $\delta$  according to (7). If the two input values  $\alpha, \beta$  are close to each other,

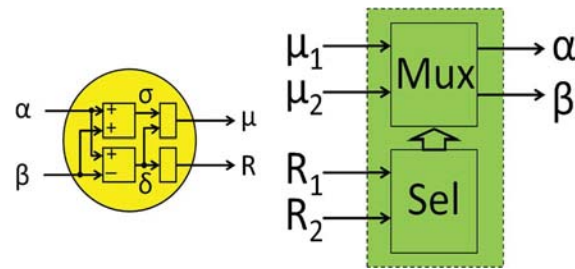


Fig. 3. (Left) Internal structure of the basic cell (bc) with reliability bit generation. (Right) Boolean selectivity mechanism: block Sel determines the output of block Mux.

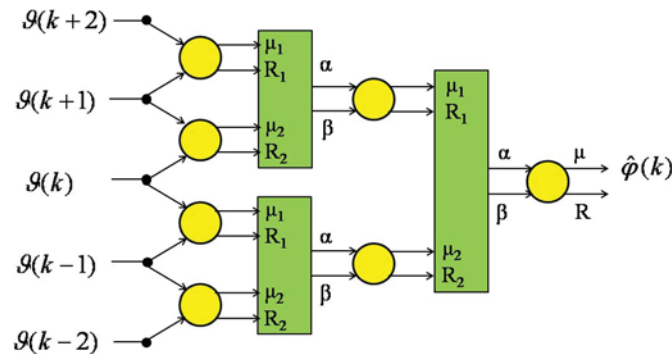


Fig. 4. Basic cell tree with inserted Boolean elements for the reliability-based selection mechanism.

the averaging result is reliable. There exist also critical combinations  $\alpha, \beta$  for which the averaging result is less certain, but these cases with  $|\delta| \approx \pi/R$  can be detected by a simple comparison of  $\delta$  with appropriate constants. Note that (7) is discontinuous at  $|\delta| = \pi/R$ , which is in accordance with a complex expression for  $\mu$  [15]. In practice, a reliability mark (single bit output  $R$ , which is not to be confused with the ray number  $R$ ) is generated in parallel with the angle output with a few Boolean elements. Each cell marks its output as reliable (small input angle difference) or less reliable (big input angle difference).

The right side of Fig. 3 shows how the reliability information is used to process the average angles. The depicted unit that receives two angles and two reliability bits has to distinguish between two cases: Both input angles have the same reliability, or one is marked as better than the other one. If both angles have equal reliability, the Mux performs the standard assignment  $\alpha = \mu_1, \beta = \mu_2$  and both values are forwarded to the following basic cell, where the normal averaging procedure is applied, and a new reliability bit is generated. Otherwise, if for example  $R_1 = 1, R_2 = 0$  indicates that the only good angle is  $\mu_1$ , it is assigned to both outputs, and the basic cell delivers  $\mu = f(\mu_1, \mu_1) = \mu_1$  with an inherited reliability mark of 1, whereas the “bad” angle  $\mu_2$  is discarded by the selectivity mechanism.

For this method, no additional calculations or modifications of the presented averaging cell are necessary, only a few Boolean operations (Sel) and a switch (Mux). Promising simulation results of this algorithm for QPSK were first published in [16] under the name selective maximum-likelihood phase approximation (SMLPA); the phase estimator has also been implemented and successfully employed in several experiments [17].

Fig. 4 shows how the two elements from Fig. 3 are combined to form a fast angle-based phase estimator. The tree structures for the phase estimator would usually have to process an odd number of input angles, namely  $2N + 1$  where  $N$  is the number of predecessors and successors around a center value. It is advantageous to design a tree for  $N = 2$  (our example, also for simulation) with multiple use one or more center value—this simple method replaces weighted complex summation that is used to optimize V&V phase estimators [15]. Intermediate values are stored in the basic cells for one clock cycle, and the Boolean selectivity mechanism operates without additional delay.

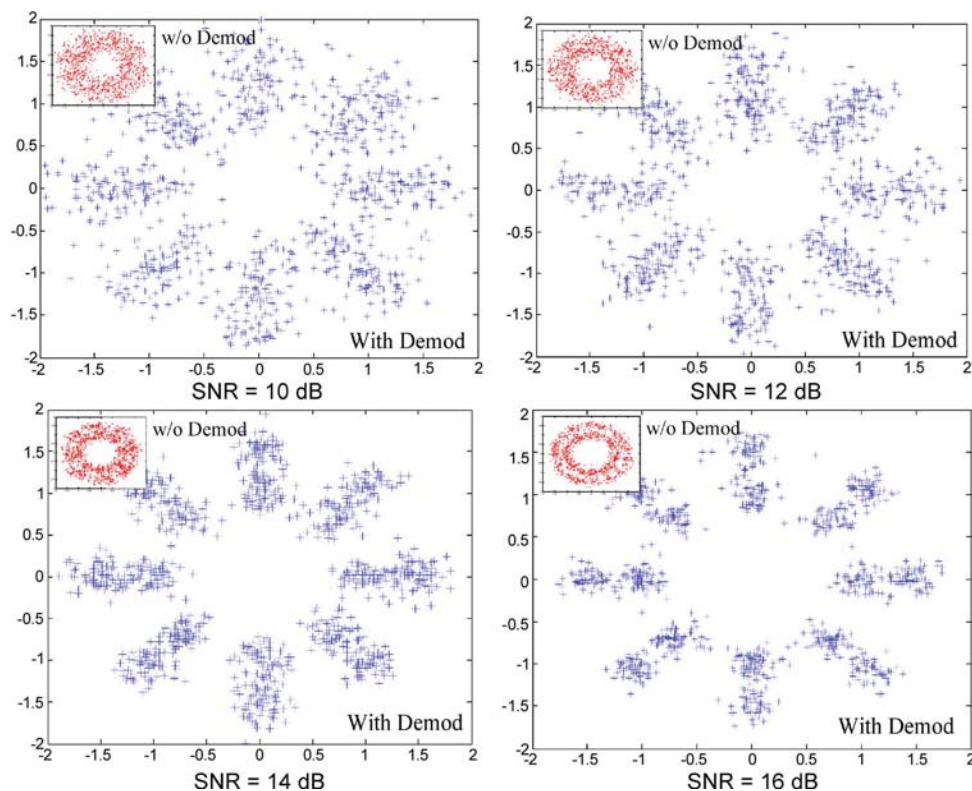


Fig. 5. Received symbols before demodulation (inset) and after demodulation ( $N = 2$ ).

## 6. Simulation Results

The functionality of the presented phase-estimation method was demonstrated with a small simulation study: A set of random 16-QAM star constellation symbols was generated, 10-GBaud coherent transmission with DFB lasers was modeled (residual frequency mismatch of 20 MHz, sum linewidth of 1 MHz), and the simulation was repeated for several optical signal-to-noise ratio values (see Fig. 5): 10 dB, 12 dB, 14 dB, and 16 dB. While the received symbols before demodulation are spread over a ring, the demodulation with the estimated phase leads to clearly separated rays corresponding to the transmitted symbols. At least for the outer ring symbols (equivalent to a 8-PSK system), a good BER performance of the decoder can be expected. The estimated phase-ambiguity problem can be solved by differential encoding and jump number generation [10] or a real-time phase-unwrapping method [15].

The magnitude of the inner ring symbols was chosen to be half of the outer ring symbols. Since the ray separation with the presented phase estimation algorithm works very well, the decoder for the amplitude modulation data recovery is supposed to be the problematic part of the QAM-16 star constellation receiver. Smaller magnitudes for the inner ring would enhance its BER performance but make the differential decoder for the phase demodulation more sensitive to noise. Optimization investigations concerning this tradeoff are still going on.

## 7. Conclusion

We have presented a general method to estimate the phase of a coherent transmission system that employs RSCs. The novel multiplier-free method was already implemented and tested for QPSK in real-time implementations [4], [6]. Theoretical derivations and explanations are illustrated by simulated receiver side constellations before and after demodulation with the estimated phase for several values of the optical SNR.

## References

- [1] R. Noé, "Phase noise tolerant synchronous QPSK/BPSK baseband-type intradyne receiver concept with feedforward carrier recovery," *J. Lightw. Technol.*, vol. 23, no. 2, pp. 802–808, Feb. 2005.
- [2] S. Savory, "Compensation of fibre impairments in digital coherent systems," presented at the Eur. Conf. Optical Commun., Brussels, Belgium, 2008, Paper Mo.3.D.1.
- [3] A. Leven, N. Kaneda, and Y. Chen, "A real-time CMA-based 10 Gb/s polarization demultiplexing coherent receiver implemented in an FPGA," in *Proc. Opt. Fiber Commun./Nat. Fiber Opt. Eng. Conf.*, 2008, pp. 1–3.
- [4] T. Pfau, R. Peveling, F. Samson, J. Romoth, S. Hoffmann, S. Bhandare, S. Ibrahim, D. Sandel, O. Adamczyk, M. Porrmann, R. Noé, J. Hauden, N. Grossard, H. Porte, D. Schlieder, A. Koslovsky, Y. Benarush, and Y. Achiam, "Polarization-multiplexed 2.8 Gbit/s synchronous QPSK transmission with real-time digital polarization tracking," presented at the Eur. Conf. Exhibition Optical Commun., Berlin, Germany, Sep. 16–20, 2007, Paper 8.3.3.
- [5] H. Sun, K. Wu, and K. Roberts, "Real-time measurements of a 40 Gb/s coherent system," *Opt. Exp.*, vol. 16, no. 2, pp. 873–879, Jan. 2008.
- [6] V. Herath, R. Peveling, T. Pfau, O. Adamczyk, S. Hoffmann, C. Wördehoff, M. Porrmann, and R. Noé, "Chipset for a coherent polarization-multiplexed QPSK receiver," presented at the Optical Fiber Commun. Conf., San Diego, CA, 2009, Paper JThA63.
- [7] P. J. Winzer, A. H. Gnauck, C. R. Doerr, M. Magarini, and L. L. Buhl, "Spectrally efficient long-haul optical networking using 112-Gb/s polarization-multiplexed 16-QAM," *J. Lightw. Technol.*, vol. 28, no. 4, pp. 547–556, Feb. 2010.
- [8] T. Pfau, S. Hoffmann, and R. Noé, "Hardware-efficient coherent digital receiver concept with feedforward carrier recovery for M-QAM constellations," *J. Lightw. Technol.*, vol. 27, no. 8, pp. 989–999, Apr. 2009.
- [9] T. Pfau, R. Peveling, V. Herath, S. Hoffmann, C. Wördehoff, O. Adamczyk, M. Porrmann, and R. Noé, "Towards real-time implementation of coherent optical communication," in *Proc. OFC/NFOEC*, Mar. 22–26, 2009, pp. 1–3.
- [10] R. Noé, "PLL-free synchronous QPSK polarization multiplex/diversity receiver concept with digital I&Q baseband processing," *IEEE Photon. Technol. Lett.*, vol. 17, no. 4, pp. 887–889, Apr. 2005.
- [11] A. J. Viterbi and A. M. Viterbi, "Nonlinear estimation of PSK-modulated carrier phase with application to burst digital transmission," *IEEE Trans. Inf. Theory*, vol. IT-29, no. 4, pp. 543–551, Jul. 1983.
- [12] S. Hoffmann, S. Bhandare, T. Pfau, O. Adamczyk, C. Wördehoff, R. Peveling, M. Porrmann, and R. Noé, "Frequency and phase estimation for coherent QPSK transmission with unlocked DFB lasers," *IEEE Photon. Technol. Lett.*, vol. 20, no. 18, pp. 1569–1571, Sep. 2008.
- [13] J. E. Volder, "The CORDIC trigonometric computing technique," *IRE Trans. Electron. Comput.*, vol. EC-8, no. 3, pp. 330–334, Sep. 1959.
- [14] M. G. Taylor, "Accurate digital phase estimation process for coherent detection using a parallel digital processor," in *Proc. Eur. Conf. Opt. Commun.*, Glasgow, U.K., 2005, pp. 263–264, Paper Tu4.2.6.
- [15] S. Hoffmann, R. Peveling, T. Pfau, O. Adamczyk, R. Eickhoff, and R. Noé, "Multiplier-free real-time phase tracking for coherent QPSK receivers," *IEEE Photon. Technol. Lett.*, vol. 21, no. 3, pp. 137–139, Feb. 2009.
- [16] S. Hoffmann, T. Pfau, O. Adamczyk, R. Peveling, M. Porrmann, and R. Noé, "Hardware-efficient and phase noise tolerant digital synchronous QPSK receiver concept," presented at the Coherent Optical Technologies Applications (COTA), Topical Meeting, OSA, Whistler, BC, Canada, Jun. 28–30, 2006, Paper CThC6.
- [17] T. Pfau, C. Wördehoff, R. Peveling, S. Ibrahim, S. Hoffmann, O. Adamczyk, S. Bhandare, M. Porrmann, R. Noé, A. Koslovsky, Y. Achiam, D. Schlieder, N. Grossard, J. Hauden, and H. Porte, "Ultra-fast adaptive digital polarization control in a realtime coherent polarization-multiplexed QPSK receiver," presented at the Optical Fiber Commun. Conf., San Diego, CA, 2008, Paper OTuM3.